

Quantum oscillations in $(\text{DMET-TSeF})_2\text{AuCl}_2$

N. Biškup* and J. S. Brooks

NHMFL—Florida State University, Tallahassee, Florida 32310

R. Kato

Institute for Solid State Physics, University of Tokyo, Roppongi, Minato-ku, Tokyo 106, Japan

K. Oshima

Department of Physics, Faculty of Science, Okayama University, Tsushima-naka, Okayama 700, Japan

(Received 22 September 1999)

We report magnetoresistance measurements to 33 T at low temperatures in dimethyl(ethylenedithio)tetraselenafulvalene $(\text{DMET-TSeF})_2\text{AuCl}_2$, an organic conductor with a strictly quasi-one-dimensional electronic structure at low temperatures. Magnetic field induced spin-density wave (FISDW) transitions, similar in origin to those observed in the Bechgaard salts, are investigated vs temperature and tilted magnetic field. Rapid oscillations (RO) of about 300 T are detected in this material, but only in the FISDW states. We conclude from this study that the reconstruction of a one-dimensional Fermi surface is a necessary condition for the RO phenomena to occur, and we describe the form of the resulting electronic structure. [S0163-1829(99)50446-3]

Low dimensional metals represent one of the fundamental areas of condensed-matter physics. In particular, quasi-one-dimensional (Q1D) metals are of interest due to the nature of the instabilities which drive the many competing ground states, and for the possibility of strong electron correlation effects. In pursuit of this, the Bechgaard salts, a class of quasi-one-dimensional organic conductors,¹ have been the subject of numerous investigations, particularly in high magnetic fields. Most prominent are magneto-oscillatory effects, observed at liquid-helium temperatures, which fall into two classes: magnetic field induced spin-density wave (FISDW) transitions, and rapid oscillations (RO). The FISDW transitions are known to come from the improvement of the nesting condition of the Q1D Fermi surface with increasing magnetic field, which causes a Fermi-surface reconstruction and produces small electron and hole pockets.¹ The quantum oscillation frequency associated with these transitions, which is of the order of 60 T, arises from the quantization of the nesting vector with quantum number N . In contrast, the origin of the RO oscillations has been controversial since in principle, a one-dimensional open Fermi surface cannot support Shubnikov–de Haas (SdH) oscillations. Experiments in tilted magnetic fields show that both the FISDW and RO frequencies follow an angular dependence which is characteristic of quasi-two-dimensional (Q2D) pockets which result from the nesting of the Q1D Fermi surface.

To accurately describe seemingly anomalous properties such as the RO phenomena, or other unusual effects which may arise,^{2,3} a proper understanding of the electronic structure of a Q1D material is essential. The Bechgaard compounds, represented by $(\text{TMTSF})_2X$, are 2:1 charge-transfer salts involving a cation TMTSF and an anion X . In all cases where the RO have been observed, a Fermi-surface reconstruction has occurred. Here the Fermi surface has been nested by one or more of three possible mechanisms: anion ordering (AO) where low-symmetry anions such as ClO_4 , ReO_4 , and NO_3 order in such a way as to double the unit

cell; spin-density wave formation (SDW) for high symmetry anions such as PF_6 and AsF_6 , where the Fermi surface nests due to a Peierls-type instability; and FISDW, as described above. The oscillation frequency of the RO is typically between 200 and 300 T, which represents about 3% of the Brillouin zone. (The small electron and hole pockets produced by the FISDW effect cannot, individually, produce such a large orbit.) Based on models for the reconstruction of the original Q1D Fermi surface, arguments for Stark effect orbits in the metallic (non-SDW) phases,⁴ and arguments for magnetic breakdown orbits in the SDW (Refs. 5 and 6) and FISDW (Ref. 7) phases, have recently been proposed. One may conclude, based on the mechanisms proposed in Refs. 4–7, that no RO effect should occur in the original Q1D Fermi-surface configuration. The present work is entirely consistent with this description.

We may gain a better understanding of the origin of the RO in Q1D systems by considering in this paper the $(\text{DMET-TSeF})_2X$ system, which, from an earlier report,⁸ exhibits FISDW behavior. We will show that the asymmetric donor DMET-TSeF system is an excellent choice to study magnetotransport mechanisms in Q1D materials. It is the first system to show FISDW states at ambient pressure without the complications of anion ordering. Hence at low temperatures, the electronic structure involves a true, metallic Q1D Fermi surface. The asymmetric cation molecule dimethyl(ethylenedithio)tetraselenafulvalene (DMET-TSeF) is similar to the symmetric TMTSF donor in the Bechgaard salts, but an additional sulfur-based aromatic ring replaces the ethylene pair on one end.⁹ The resulting Q1D Fermi surface is, however, very similar to that of the Bechgaard salts due to the linear stacking of the planar cations along the crystalline a axis. For linear anions such as $X = \text{AuI}_2$, AuCl_2 , and I_3 there is no anion ordering transition, no Peierls-like instability at low temperatures, and except for AuI_2 ($T_c = 0.58$ K), no evidence for superconductivity to 40 mK.

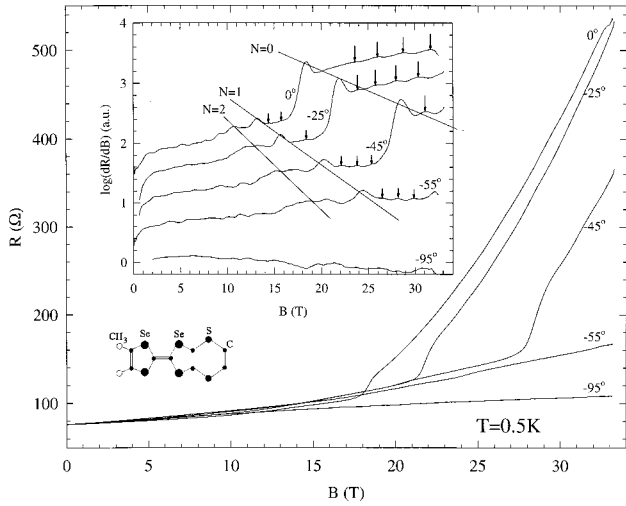


FIG. 1. Resistance vs magnetic field of $(\text{DMET-TSeF})_2\text{AuCl}_2$ for selected field directions (angle measured from the b axis) at 0.5 K. Inset: First derivative of magnetoresistance data (offset for clarity). The lines indicate the field positions of FISDW transitions and the arrows indicate the field positions of rapid oscillations. The DMET-TSeF donor molecule is also shown.

Hence these materials are Q1D metals at low temperatures,⁹ and only the FISDW mechanism produces a Fermi-surface reconstruction.

The relationship between the properties of $(\text{DMET-TSeF})_2\text{AuCl}_2$ and the Bechgaard salts have been examined by performing electrical transport measurements on several single crystals of $(\text{DMET-TSeF})_2\text{AuCl}_2$ over a wide range of temperature and magnetic field. (The synthesis of the samples, which are typically less than $0.5 \times 0.1 \times 0.1$ mm in size, is described in Ref. 9.) A standard 4-probe technique, with $12.5 \mu\text{m}$ gold wire and paint, was employed with an ac current ($10 \mu\text{A}$) and voltage measured along the most conducting a axis. The magnetic field was applied at an angle θ with respect to the least conducting direction b (which corresponds to the c axis in Bechgaard salts). All samples measured exhibited similar behavior.

The magnetoresistance (MR) data for selected magnetic-field directions with respect to the b axis at $T=0.5$ K are shown in Fig. 1. The largest changes in the MR above 15 T reflect the transition to the $N=0$ FISDW state. From the derivatives of the MR data (see insets of Figs. 1 and 3), the FISDW phase transitions are clearly discernible, and consistent with previous studies.⁸ Application of the Onsager relation to the FISDW transitions, which are periodic in inverse field, yields a frequency of $F_{\text{SDW}}=48 \pm 5$ T for $\theta=0^\circ$. This is slightly less than the value (~ 60 T) seen in the Bechgaard salts. From this frequency and the extrapolation of the existing FISDW transition fields, we find that the transition at 18.4 T is the final, $N=0$ FISDW transition. In separate measurements in the millikelvin range (Fig. 3 inset), we have observed successive transitions down to 6.5 T ($N=6$).

The most important experimental result of the present work is the observation, in the $(\text{DMET-TSeF})_2\text{X}$ system, of RO quantum oscillations. They are evident in the MR derivatives in Fig. 1, particularly in the $N=0$ state. In the low temperature data (Fig. 3 inset) the RO are evident in the higher index subphases. We have determined that the RO

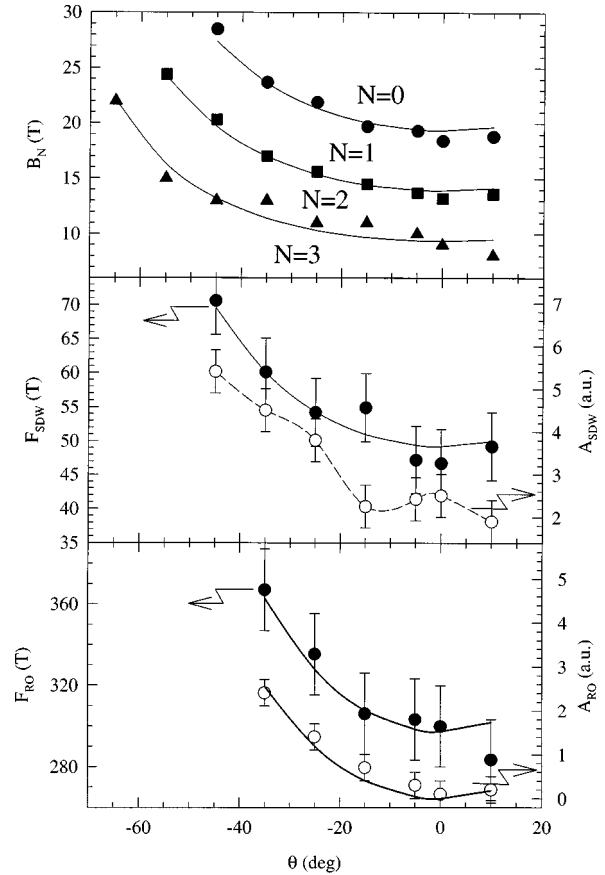


FIG. 2. Angular dependence of quantum oscillation phenomena. (a) $N=0, 1, 2$ FISDW transitions (B_N) as a function of angle (θ). (b) The FISDW frequency (F_{SDW}) and $N=0$ A_{SDW} amplitude vs angle (θ). The dashed line is a guide to the eye. (c) RO frequency (F_{RO}) and RO amplitude (A_{RO}) vs angle (θ). The solid lines represent fits to $1/\cos(\theta)$ behavior.

appear only in the FISDW states, that is, no periodic oscillations have been seen at angles for which FISDW state is not detected. The RO frequency for $\theta=0^\circ$ is 300 ± 20 T which is again very similar to the RO in Bechgaard salts. It amounts to 3.8% of the first Brillouin zone.

The angular dependence of the $N=0, 1,$ and 2 FISDW transitions, the corresponding frequency F_{SDW} , and the RO frequency (F_{RO}) are shown in Figs. 2(a), (b), and (c), respectively. All data can be fitted well to a $1/\cos(\theta)$ dependence, showing that the origin of the effects are orbital (i.e., arise from Q2D pockets), as in the case of Bechgaard salts. In Figs. 2(b) and (c) we also plot the amplitudes A_{SDW} and A_{RO} as a function of angle for the $N=0$ FISDW transition and the 13th RO Landau level, respectively. Both A_{SDW} and A_{RO} show a similar orbital dependence, which increases with θ . A similar behavior for the FISDW transitions in $(\text{TMTSF})_2\text{ClO}_4$ has been reported by Boeinger *et al.*¹⁰ The increase in amplitude of the FISDW and RO features with angle may imply that, in addition to the simple model of a Q2D pocket topology, there are some aspects of the transport which depend on finite carrier momentum in the least conducting direction. This seems to be the case, even though the orbital frequencies seem to faithfully follow the $1/\cos(\theta)$ dependence. We note that $(\text{DMET-TSeF})_2\text{AuCl}_2$ also exhibits an oscillatory angular dependent magnetoresistance (AMRO)

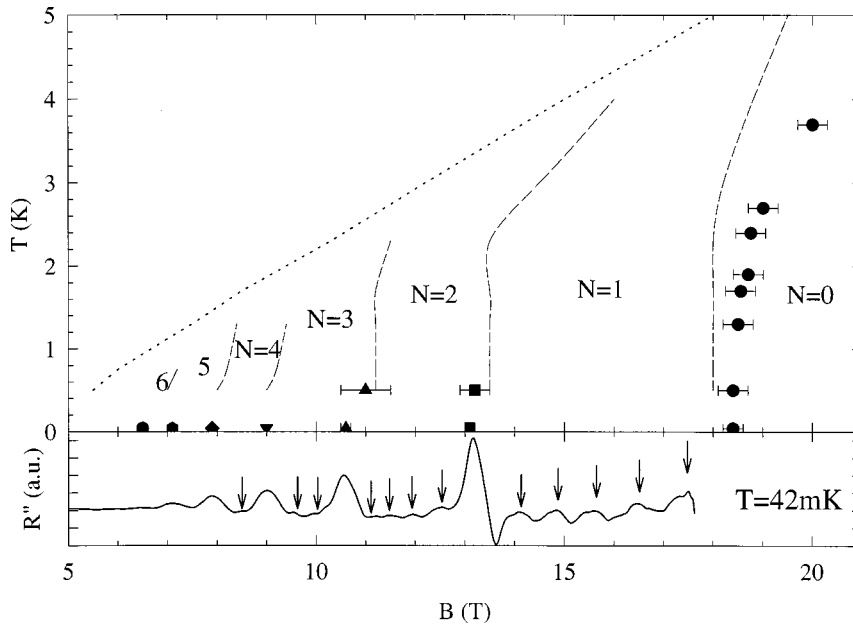


FIG. 3. Upper panel: Temperature–magnetic-field (TB) phase diagram for FISDW states. Symbols: $(\text{DMET-TSeF})_2\text{AuCl}_2$. The dashed lines and dotted line: first-order subphase transitions and second-order metal-FISDW transitions, respectively, in $(\text{TMTSF})_2\text{PF}_6$ (after Ref. 12). Lower panel: the lowest temperature, high-index FISDW data. Here R'' is the second derivative of the MR with respect to field. The RO (tick marks) are visible in the FISDW subphases for $N \leq 3$ in R'' .

effect^{8,11} and further work will be needed to determine if this might influence the behavior of A_{SDW} and A_{RO} .

The T - B phase diagram for $(\text{DMET-TSeF})_2\text{AuCl}_2$ is shown in Fig. 3, as derived from the field position of the FISDW transitions in the high field data and also from the 40 mK results. For comparison, we also show the corresponding phase diagram of $(\text{TMTSF})_2\text{PF}_6$ material at a pressure of 8 kilobars, taken from Ref. 12. There is a striking, nearly one-to-one, correspondence between the two systems. This similarity is even stronger if we note that $(\text{TMTSF})_2\text{PF}_6$ does not have anion ordering, and a pressure of 8 kilobars removes the ambient pressure Peierls-like SDW state. Hence the FISDW states in both cases in Fig. 3 arise from the original Q1D Fermi surface. Further work is necessary to connect the 40 mK part of the phase diagram with the higher temperature data at lower fields. We can only note that in the present work, no FISDW with index above $N=3$ was observed at

0.5 K. Hence the second-order phase boundary which separates the metallic and FISDW states may be lower in $(\text{DMET-TSeF})_2\text{AuCl}_2$ than in $(\text{TMTSF})_2\text{PF}_6$ (see dotted line in Fig. 3).

A further comparison with the Bechgaard salts involves the temperature dependence of the RO amplitudes, as shown in Fig. 4. The RO amplitude for $(\text{DMET-TSeF})_2\text{AuCl}_2$ increases monotonically with decreasing T . In the ambient pressure SDW states of the Bechgaard salts, the RO amplitudes show a maximum in the range 2–4 K, and generally vanish at the lowest temperatures.⁶ In contrast, even at 40 mK we are able to observe RO (see lower panel in Fig. 3). In the FISDW states of the Bechgaard salts the RO amplitudes can have a more complicated behavior. However, in the case of $(\text{TMTSF})_2\text{ClO}_4$ in the high field state above 30 T, which is believed to be in the final $N=0$ state, the RO amplitudes also increase monotonically with decreasing temperature.¹³ In the

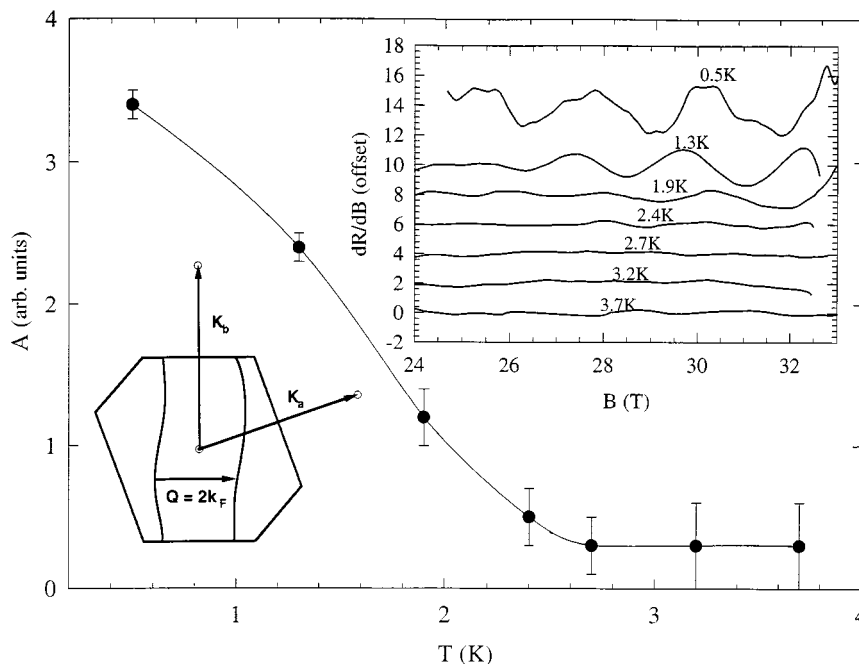


FIG. 4. RO amplitude (A_{RO}) vs temperature (T). The line is a guide to the eye. Inset 1: oscillatory part of the magnetoresistance (curves offset). Inset 2: Fermi surface for $(\text{DMET-TSeF})_2\text{AuCl}_2$ (after Ref. 9).

event that there are no subphases, and no further improvements in the nesting condition, a monotonic increase in quantum oscillation amplitudes would be expected with decreasing temperature.¹⁴

Because of the topology of the Q1D Fermi surface (see inset of Fig. 4), the only nesting vector which can gap most of the Q1D band is $\mathbf{Q} \approx 2\mathbf{k}_F$, where \mathbf{k}_F is some average over the b axis dispersion since the nesting is not perfect. The imperfect nesting produces the small pockets associated with the FISDW state. In addition, by standard Brillouin zone-folding methods with the new \mathbf{Q} vector periodicity,⁶ magnetic breakdown orbits with extremal areas of order 1–3% of the original Brillouin zone will appear in the reconstructed Fermi-surface topology. A precise assignment of \mathbf{Q} will require a microscopic probe, such as NMR.

To summarize, we have shown that the asymmetric donor DMET-TSeF system is an ideal system to study Q1D mechanisms at low temperatures and in high magnetic fields. We have constructed a T - B phase diagram which is almost identical to the one for $(\text{TMTSF})_2\text{PF}_6$ under critical pressure. We have observed RO in the FISDW state in this material. However, the RO is absent in the metallic state, i.e., below the FISDW threshold field. This is in contrast to the cases of $(\text{TMTSF})_2\text{ClO}_4$ and $\text{TMTSF}_2\text{ReO}_4$ which both undergo anion ordering and have Fermi-surface reconstructions in their

metallic states. Based on current experiments and models^{4–7} for RO in either the metallic or SDW/FISDW states, we conclude that a Fermi-surface reconstruction of a Q1D Fermi surface is necessary to provide orbits for the RO mechanism. We further note that the FISDW transitions in the title material are not preceded by superconductivity (at least to 40 mK), hence superconductivity is not a necessary prerequisite for the FISDW phenomena. And finally, the temperature dependence of the RO amplitudes is monotonic with temperature—hence there are no subphases or further changes in electronic structure within the final $N=0$ FISDW state in $(\text{DMET-TSeF})_2\text{AuCl}_2$ in line with the expectations of the standard theoretical model for FISDW behavior.¹ This underscores the point that the title material provides perhaps the best example of a true Q1D metal.

Note added in proof. Very recent measurements in the vicinity of the phase boundary near 7 K above 25 T give some indication of quantum oscillation behavior. Further work is planned in the high temperature range well above the phase line in fields of up to 45 T to try to resolve this behavior.

This work was supported by Grant No. NSF-DMR-95-10427. The NHMFL is supported through a contractual agreement between the NSF through Grant No. NSF-DMR-95-27035 and the State of Florida.

*Author to whom correspondence should be addressed. Electronic address: biskup@magnet.fsu.edu

¹For an excellent review of the current experimental and theoretical status of the Bechgaard salts see T. Ishiguro, K. Yamaji, and G. Saito, *Organic Superconductors II* (Springer-Verlag, Berlin, 1998).

²G. M. Danner and P. M. Chaikin, *Phys. Rev. Lett.* **75**, 4690 (1995).

³S. P. Strong, D. G. Clarke, and P. W. Anderson, *Phys. Rev. Lett.* **73**, 1007 (1994).

⁴S. Uji *et al.*, *Solid State Commun.* **103**, 387 (1997).

⁵S. Uji *et al.*, *Phys. Rev. B* **55**, 12 446 (1997).

⁶J. S. Brooks *et al.*, *Phys. Rev. B* **59**, 2604 (1999).

⁷S. Uji *et al.*, *Synth. Met.* **86**, 1909 (1997).

⁸K. Oshima *et al.*, *Synth. Met.* **70**, 861 (1995).

⁹R. Kato *et al.*, *Synth. Met.* **61**, 199 (1993).

¹⁰G. S. Boebinger *et al.*, *Phys. Rev. Lett.* **64**, 591 (1990).

¹¹N. Biskup *et al.* (unpublished).

¹²J. R. Cooper *et al.*, *Phys. Rev. Lett.* **63**, 1984 (1989).

¹³J. S. Brooks *et al.*, *Phys. Rev. B* **53**, 14 406 (1996).

¹⁴D. Shoenberg, *Magnetic Oscillations in Metals* (Cambridge University Press, Cambridge, 1994).